Journal of Bioenergetics and Biomembranes, Vol. 37, No. 6, December 2005 (© 2005)
DOI: 10.1007/s10863-005-9489-5

Chemomechanical Coupling in Single-Molecule F-Type ATP Synthase

Ryota Iino,[1] Yannick Rondelez,[1] Masasuke Yoshida,[2] and Hiroyuki Noji[1,3]

An extremely small reaction chamber with a volume of a few femtoliters was developed for a highly sensitive detection of biological reaction. By encapsulating a single F_1-ATPase (F_1) molecule with ADP and an inorganic phosphate in the chamber, the chemomechanical coupling efficiency of ATP synthesis catalyzed by reversely rotated F_1 was successfully determined (Rondelez *et al*., 2005a, *Nature*, **444**, 773–777). While the $\alpha_3\beta_3\gamma$ subcomplex of F_1 generated ATP with a low efficiency (∼10%), inclusion of the ε subunit into the subcomplex enhanced the efficiency up to 77%. This raises a new question about the mechanism of F_0F_1-ATP synthase (F_0F_1): How does the ε subunit support the highly coupled ATP synthesis of F_1? To address this question, we measured the conformational dynamics of the ε subunit using fluorescence resonance energy transfer (FRET) at the single-molecule level. The experimental data revealed ε changes the conformation of its C-terminus helices in a nucleotide-dependent manner. It is plausible that the conformational change of ε switches the catalytic mode of F_0F_1 for highly coupled ATP synthesis.

KEY WORDS: F_0F_1-ATP synthase; F_1-ATPase; rotary molecular motor; single-molecule imaging; single-molecule manipulation; magnetic tweezers; chemomechanical coupling; microfabrication; polydimethylsiloxane; fluorescence resonance energy transfer.

F_1-ATPase: A HIGHLY EFFICIENT ROTARY MOTOR DRIVEN BY ATP HYDROLYSIS

F_1-ATPase (F_1) is a rotary molecular motor composed of protein (Noji *et al*., 1997). The subunit composition of bacterial F_1 is $\alpha_3\beta_3\gamma\delta\varepsilon$, and its $\alpha_3\beta_3\gamma$ subcomplex is the minimum functional unit as a motor (Fig. 1(A), *top*). The stator and rotor parts are formed by the $\alpha_3\beta_3$ ring and γ subunit, respectively. Each β subunit carries a catalytic nucleotide-binding site. Consistent with the crystal structure of the $\alpha_3\beta_3\gamma$ subcomplex in which the three α and β subunits are alternately arranged (Abrahams *et al*., 1994), single-molecule imaging revealed that it makes a stepping rotation of 120° (Yasuda *et al*., 1998). A statistical analysis of the dwell time between the 120° steps strongly suggests that each step is driven by single ATP hydrolysis; the chemomechanical coupling ratio is three ATP molecules per turn.

Although extensive studies on the ATP hydrolysis activity and ATP-driven rotation of F_1 have been conducted, its physiological role is ATP synthesis (Boyer, 1997; Pedersen, 1996). In vivo, F_1 forms a holoenzyme complex of F_0F_1-ATP synthase (F_0F_1) together with membrane-embedded rotary motor F_0 (Fig. 1(A), *bottom*). F_0 rotates its rotor ring using proton flux driven by the proton motive force across the membrane. With regard to the ATP synthesis reaction, it is widely accepted that when F_0 forcibly reverses the rotation of F_1, the chemical reaction is also reversed to generate ATP from ADP and an inorganic phosphate. This notion was experimentally supported by Itoh *et al*. (2004) who first demonstrated that the reverse rotation of the $\alpha_3\beta_3\gamma$ subcomplex of F_1 led to ATP

[1] The Institute of Scientific and Industrial Research, Osaka University, Osaka, Japan.
[2] Chemical Resources Laboratory, Tokyo Institute of Technology, Yokohama, Japan.
[3] To whom correspondence should be addressed; e-mail: hnoji@sanken.osaka-u.ac.jp.

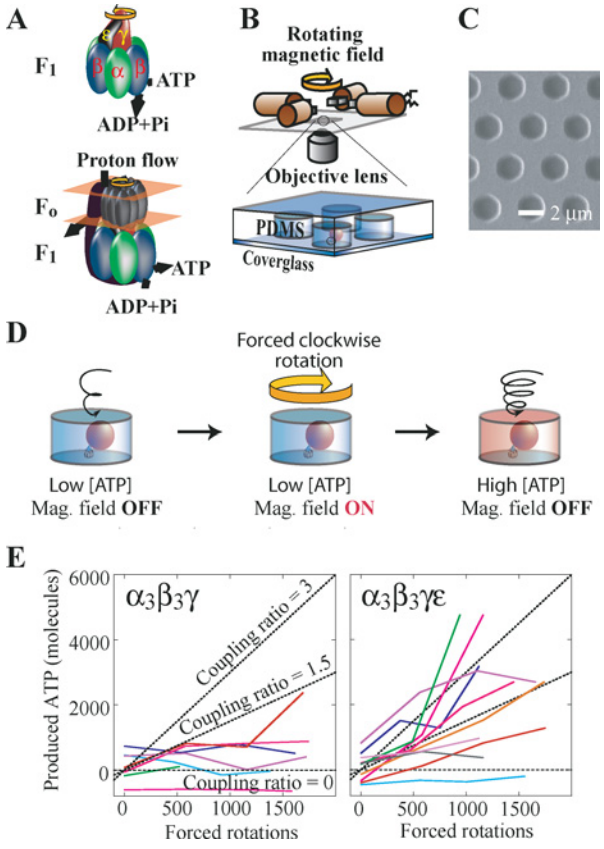

Fig. 1. Single-molecule experiment of ATP synthesis by forced rotation of F_1. (A) Schematic structures of F_1 (*top*) and F_0F_1 (*bottom*). F_1 rotates anticlockwise by ATP hydrolysis, and proton-driven F_0 rotates F_1 clockwise for ATP synthesis. (B) Schematic drawing of the experimental set up. (C) Scanning electron microscopic image of the chamber array. (D) Experimental procedure of ATP synthesis. (*left*) Active single F_1 is enclosed in a femtoliter chamber. (*center*) A magnetic bead attached to γ is rotated clockwise using magnetic tweezers. Newly synthesized ATP is entrapped in the chamber. (*right*) The number of ATP molecules in the chamber is estimated from the ATP-driven rotational speed. (E) The number of ATP synthesized by $\alpha_3\beta_3\gamma$ (*left*) and $\alpha_3\beta_3\gamma\varepsilon$ (*right*) subcomplexes of F_1 after forced rotation. Each trace belongs to individual F_1. Dotted lines indicate slopes of the expected chemomechanical coupling ratios: 3 for 100% efficiency; 1.5 for 50% efficiency; and 0 for 0% efficiency.

synthesis. However, without knowing the number of active F_1 molecules in the reaction chamber, it was difficult to determine the number of ATP molecules synthesized per turn and per F_1 molecule.

F_1 SYNTHESIZES ATP WITH HIGH EFFICIENCY WHEN THE ROTATION IS REVERSED

Because of the reasons mentioned earlier, it is essential to measure the ATP synthesis activity of an active F_1 molecule individually to know the efficiency of chemomechanical coupling. To achieve this, a major problem is that the expected amount of synthesized ATP is extremely small. Even when the efficiency is assumed to be 100% (three ATP molecules/turn), the reverse rotation at 10 Hz for 1 min yields only 1800 ATP molecules, which is far below the limit of conventional ATP-detection methods such as a lucifearase assay. However, if all ATP molecules produced are accumulated in a very small volume, such as 6 fL ($=\{1.8\,\mu\mathrm{m}\}^3$), this mechanically reversed rotation should increase the ATP concentration by 0.5 μM. To make a micron-sized reaction chamber, a polydimethylsiloxane (PDMS) sheet with a large number of microcavities was prepared by conventional microfabrication methods (Fig. 1(C)). The sheet was placed on a coverglass to construct the femtoliter chambers. A sample solution sandwiched between the sheet and the glass is hermetically entrapped in the chambers (Rondelez *et al.*, 2005b). Thus, an F_1 molecule was encapsulated in a femtoliter chamber (Rondelez *et al.*, 2005a).

Figure 1(D) shows the experimental procedures of the single-molecule ATP synthesis. First, an active F_1 molecule was identified as a rotating particle at a very low ATP concentration (200 nM) in the presence of ADP (100 μM) and phosphate (10 mM). It was enclosed in the chamber, followed by reverse rotation at 10 Hz for 1 min using magnetic tweezers, and was released from the tweezers. Newly synthesized ATP molecules were accumulated in the chamber and when released from tweezers, F_1 resumed ATP-hydrolysis driven rotation. It should be noted that the rotational speed is proportional to the ATP concentration at such low ATP concentrations. Therefore, the number of synthesized ATP molecules can be determined from the increase in the rotational speed before and after forced reverse rotation. In contrast to our expectation, the efficiency of the $\alpha_3\beta_3\gamma$ subcomplex was very low—only ~10% of theoretical efficiency (3ATP/one reverse revolution) (Fig. 1(E), *left*). However, when the ε subunit was reconstituted with $\alpha_3\beta_3\gamma$, the efficiency increased significantly (Fig. 1(E), *right*). Some molecules exhibited a very high efficiency—almost 100%—with an average value of 77%. This result clearly indicates that F_1 requires the ε subunit for efficient ATP synthesis, as suggested before (Cipriano *et al.*, 2002).

SINGLE-MOLECULE IMAGING OF THE CONFORMATIONAL DYNAMICS OF ε

The ε subunit is a small subunit (~14 kDa) and rotates together with the γ subunit (Kato-Yamada *et al.*, 1998). How does it assist highly coupled ATP synthesis?

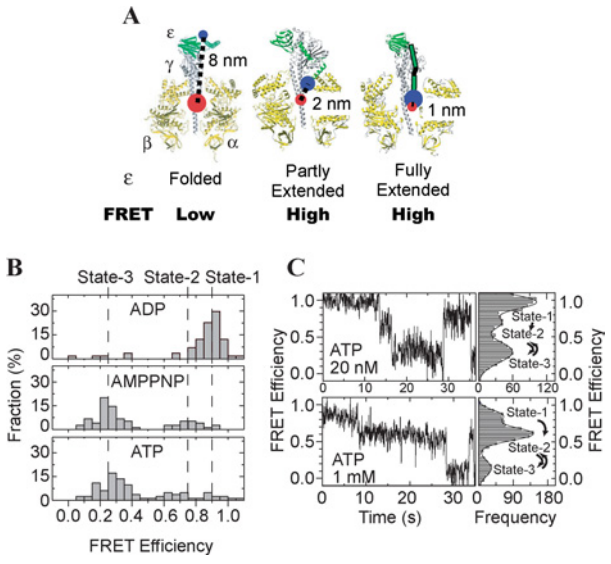

Fig. 2. Probing the conformational dynamics of the ε subunit by single-molecule FRET. (A) Structural models of the ε subunit (green) in F_1 from *E. coli* (*center*) (Hausrath *et al*., 2001; Rodgers and Wilce, 2000), thermophilic *Bacillus* PS3 (*right*) (Shirakihara *et al*., unpublished data), and δ from bovine mitochondria (*left*, equivalent to the bacterial ε) (Gibbons *et al*., 2000). The positions of the donor and acceptor dyes are indicated by red and blue circles. (B) Distributions of FRET efficiency in 1 mM ADP (*top*), AMPPNP (*middle*), and ATP (*bottom*). *C*, Examples of repetitive changes in the FRET efficiency in 20 nM (*top*) and 1 mM ATP (*bottom*).

This question is crucial for understanding the molecular mechanism of ATP synthesis. The crystal structure of the $\alpha_3\beta_3\gamma\varepsilon$ subcomplex (Gibbons *et al*., 2000) shows that ε stabilizes the protruding part of γ that is disordered in the crystal structure of the $\alpha_3\beta_3\gamma$ subcomplex (Abrahams *et al*., 1994). The stabilized part includes a part of the direct contact interface with the β and γ subunits; therefore, it is possible that this stabilization contributes to the mechanical linkage between γ and β, resulting in well-coupled ATP synthesis.

Recent progress in studies on the ε subunit indicates an alternative or/and additional explanation. Structural studies revealed that the C-terminal two α helices in the ε subunit can adopt different conformations, "hair-pin folded" and "partly-" or "fully extended" forms (Fig. 2) (Gibbons *et al*., 2000; Hausrath *et al*., 2001; Rodgers and Wilce, 2000; Shirakihara *et al*., unpublished data). Previous crosslinking experiments suggested that a conformational change of ε switches this enzyme from an ATP hydrolysis to synthesis mode (Bulygin *et al*., 2004; Kato-Yamada *et al*., 2000; Suzuki *et al*., 2003; Tsunoda *et al*., 2001). Furthermore, our ensemble-molecules FRET measurement directly revealed that ε in F_1 undergoes a large, reversible conformational change (Iino *et al*., 2005).

In order to investigate the conformational states of the ε in more detail, we recently carried out the single-molecule FRET measurement (Ha, 2001; Iino *et al*., 2005). A donor–acceptor pair was introduced in the N and C termini of the γ and ε subunits, respectively (Fig. 2(A)). The distributions of the FRET efficiency of individual F_1 molecules are shown in Fig. 2(B). In the presence of ADP, most molecules exhibited high FRET efficiency around 0.9 (Fig. 2(B), *top*, State-1), which presumably corresponds to the fully extended form (Fig 2(A), *right*). However, in the presence of AMPPNP, a non-hydrolyzing ATP analog, the FRET efficiency was separated into two populations with peaks around 0.75 or 0.25 (Fig. 2(B), *middle*, State-2 and State-3), which likely correspond to the partly extended and hair-pin folded forms (Fig. 2(A), *center* and *left*). In ATP (Fig. 2(B), *bottom*), the distribution was similar to that in AMPPNP, while some molecules exhibited repeated transitions of the FRET efficiency between State-2 and State-3 (Fig. 2(C)), indicating that F_1 occasionally alters the conformation of the ε during the ATP-driven rotation. The correlation of the conformational state of the ε and the highly coupled ATP synthesis has not yet been established. Simultaneous measurements of the single-molecule FRET with the rotation of γ will provide deeper insights, such as the role of the conformational states and dynamics of the ε for the efficiency of chemomechanical coupling in F_0F_1.

REFERENCES

Abrahams, J. P., Leslie, A. G., Lutter, R., and Walker, J. E. (1994). *Nature* **370**, 621–628.
Boyer, P. D. (1997). *Annu. Rev. Biochem.* **66**, 717–749.
Bulygin, V. V., Duncan, T. M., and Cross, R. L. (2004). *J. Biol. Chem.* **279**, 35616–35621.
Cipriano, D. J., Bi, Y., and Dunn, S. D. (2002). *J. Biol. Chem.* **277**, 16782–16790.
Gibbons, C., Montgomery, M. G., Leslie, A. G., and Walker, J. E. (2000). *Nat. Struct. Biol.* **7**, 1055–1061.
Ha, T. (2001). *Methods* **25**, 78–86.
Hausrath, A. C., Capaldi, R. A., and Matthews, B. W. (2001). *J. Biol. Chem.* **276**, 47227–47232.
Iino, R., Murakami, T., Iizuka, S., Kato-Yamada, Y., Suzuki, T., and Yoshida, M. (2005). *J. Biol. Chem.* **280**, 40130–40134.
Itoh, H., Takahashi, A., Adachi, K., Noji, H., Yasuda, R., Yoshida, M., and Kinosita, K. (2004). *Nature* **427**, 465–468.
Kato-Yamada, Y., Noji, H., Yasuda, R., Kinosita, K. Jr., and Yoshida, M. (1998). *J. Biol. Chem.* **273**, 19375–19377.
Kato-Yamada, Y., Yoshida, M., and Hisabori, T. (2000). *J. Biol. Chem.* **275**, 35746–35750.
Noji, H., Yasuda, R., Yoshida, M., and Kinosita, K., Jr. (1997). *Nature* **386**, 299–302.
Pedersen, P. L. (1996). *J. Bioenerg. Biomembr.* **28**, 389–395.

Rodgers, A. J., and Wilce, M. C. (2000). *Nat. Struct. Biol.* **7**, 1051–1054.
Rondelez, Y., Tresset, G., Nakashima, T., Kato-Yamada, Y., Fujita, H., Takeuchi, S., and Noji, H. (2005a). *Nature* **433**, 773–777.
Rondelez, Y., Tresset, G., Tabata, K. V., Arata, H., Fujita, H., Takeuchi, S., and Noji, H. (2005b). *Nat. Biotechnol.* **23**, 361–365.
Suzuki, T., Murakami, T., Iino, R., Suzuki, J., Ono, S., Shirakihara, Y., and Yoshida, M. (2003). *J. Biol. Chem.* **278**, 46840–46846.
Tsunoda, S. P., Rodgers, A. J., Aggeler, R., Wilce, M. C., Yoshida, M., and Capaldi, R. A. (2001). *Proc. Natl. Acad. Sci. U.S.A.* **98**, 6560–6564.
Yasuda, R., Noji, H., Kinosita, K., Jr., and Yoshida, M. (1998). *Cell* **93**, 1117–1124.